JACS
JOURNAL OF THE AMERICAN CHEMICAL SOCIETY

Communication

pubs.acs.org/JACS

Unraveling the Coupling between Demixing and Crystallization in Mixtures

Caroline Desgranges and Jerome Delhommelle*

Department of Chemistry, University of North Dakota, Grand Forks, North Dakota 58201, United States

Supporting Information

ABSTRACT: Using molecular simulation, we shed light on the coupling between the two nonequilibrium processes of demixing and crystallization in mixtures of fully miscible, size-matched, liquid metals. We show that the competition between these processes has a strong impact on the crystallization pathway, leading to the formation of crystal nuclei with large excesses (up to 95%) in the component of higher cohesive energy, and resulting in increases of more than 30% in the free energy barrier of nucleation. The competition between demixing and crystallization goes on to impact the growth process, as shown by the large variations in composition observed at the surface and inside the growing crystallite.

Crystallization is a fascinating nonequilibrium process, with many applications in fields as diverse as chemistry, physics, biology, and materials science.[1,2] Its complexity arises from the interplay between kinetic and thermodynamic effects,[3,4] often resulting in unexpected structures and unusual phenomena. For instance, the crystallization from a melt may lead to the formation of metastable, previously unknown, polymorphs[5] or follow unexpected nucleation pathways involving a liquid−liquid phase transition.[6−9] Elucidating the pathway to crystallization becomes even more challenging when another nonequilibrium process takes place at the same time, resulting in a coupling of this nonequilibrium process with crystallization. This is the case when the crystallizing liquid is subjected to an external field (e.g., to a shear flow or to an electric field). It has also been suggested that phase separation is yet another nonequilibrium process that can potentially compete with the crystallization process. Work in this area has focused so far on polymer blends,[10−13] with one component being a crystalline polymer and the other a noncrystalline (amorphous) polymer. It was reported that the noncrystalline polymer was rejected from the growing crystal, providing evidence of the competition between crystallization and phase separation in such systems. It remains to be seen, however, if a similar phenomenon exists in liquid mixtures and solutions, in which many of the practical applications of crystallization occur. Determining if such a coupling exists in liquid mixtures and how this could impact the mechanisms underlying crystal nucleation and growth in these systems is the aim of this work.

Metal nanocrystals and nanostructures are currently the focus of intense research because of their applications, e.g. as DNA/protein markers,[14,15] drug carriers,[16] in high-density magnetic recording,[17] and in catalysis. In particular, bimetallic nanoparticles have been shown to exhibit enhanced catalytic properties.[18] These enhanced properties result from the synergistic effects that arise upon alloying different elements in a nanoparticle. The properties of the bimetallic nanoparticles can also be, in principle, better fine-tuned by varying the composition of the nanoalloys. However, as discussed by Zheng et al.,[19] our ability to control the properties of nanoparticles is currently limited by our lack of understanding of the microscopic mechanisms underlying the formation of these materials.

In this Communication, we unravel the coupling between demixing and crystallization in liquid mixtures of metals cooled below their melting points. Using molecular simulations, we study the crystal nucleation and growth from undercooled liquid mixtures of Pd and Ag and examine the entire range of composition for this bimetallic mixture. These mixtures are especially suited to allow us to understand the interplay between crystallization and demixing. This is because the two metals are fully miscible, with similar sizes (the size mismatch is less than 5%),[20] and form solid solutions as their bulk crystalline phase. This means that any change in the local composition of the nanocrystallite will directly result from the competition between crystallization and demixing. In our simulations, we use a quantum corrected many-body potential[21] to model Pd, Ag, and their mixtures. Prior work has shown that this potential accurately predicts the thermodynamic properties of these mixtures in the liquid and in the solid phase, including the values and variations of the melting point as a function of the composition of the mixture.[22] Simulations of crystal nucleation are carried out using the umbrella sampling technique,[23] together with an order parameter measuring the amount of crystalline order in the liquid[24] (experimental work by Gasser et al. has shown that this order parameter is a reliable measure of the progress of the crystal nucleation process[25]). The umbrella sampling simulations consist in generating configurations of the liquid for a given value of the order parameter. By gradually increasing the value of the order parameter, we are able to increase the order within the liquid and to form a crystal nucleus from the liquid. This method was previously applied to simulate the nucleation process in colloidal suspensions[26] and pure metals[27] and to shed light on the polymorph selection process.[28] This approach was also recently extended to study the crystal nucleation process in binary mixtures.[29,30] Once we have obtained configurations containing a crystal nucleus of a critical size,

Received: January 20, 2014
Published: February 25, 2014

   dx.doi.org/10.1021/ja500621m | J. Am. Chem. Soc. 2014, 136, 8145−8148

we embed them in a large liquid matrix and study their evolution during unconstrained, conventional, molecular dynamics simulations.[31] We repeated this process 30 times and checked that half of the molecular dynamics trajectories (50 ± 7%) lead to the growth of the nuclei, while the other half of the trajectories resulted in the dissolution of the nuclei in the liquid. This allows us to establish that the critical nuclei we have formed are *genuine* critical nuclei. Furthermore, the analysis of the growth trajectories provides direct insight in the crystal growth mechanism.

Throughout the nucleation process, we calculate the variation in Gibbs free energy as a function of the order parameter. We present in Figure 1 the Gibbs free energy profiles obtained for all mixture compositions. All results are obtained at the same degree of undercooling for all compositions, i.e. at temperatures 35% below their respective melting points. We also include in Figure 1 results for the nucleation of pure Pd and Ag. In all cases, the starting point for our simulations is an undercooled liquid with no noticeable crystalline order, as evidenced by the low values for the order parameter (see on the left of Figure 1). Then, nucleation proceeds as the order parameter increases, leading to an increase in the Gibbs free energy. Once a crystalline nucleus of a critical size has formed (around a value of the order parameter of 0.085), the Gibbs free energy reaches a maximum (on the right of Figure 1), corresponding to the top of the free energy barrier of nucleation, ΔG_{nucl}. Nucleation from the undercooled melt leads to roughly the same ΔG_{nucl} ($28 \pm 2\ k_BT$) for pure Pd and Ag. Since the two metals are fully miscible and have similar sizes, we would expect ΔG_{nucl} to remain close to this value over the whole composition range. While this is the case for mixtures predominantly composed of Pd, Figure 1 shows a strong, unexpected, dependence on the mixture composition for mixtures with a low mole fraction in Pd. This can be best seen in Figure 1 for mixtures with Pd mole fractions of 0.2−0.4, which exhibit ΔG_{nucl} of $38 \pm 2\ k_BT$.

What is the phenomenon resulting in this steep increase in ΔG_{nucl}? Is this increase due to a dramatic change in the properties of the critical nucleus at low mole fractions in Pd? To address this issue, we closely examine the size, structure, and composition of the critical nuclei over the whole composition range. In terms of size, the critical nuclei, obtained from the different liquid mixtures, are remarkably similar to one another and all contain a total number of atoms equal to 220 ± 10. In terms of structure, the structural analysis of the critical nuclei reveals that, for all compositions, the critical nuclei are also very similar. They all are predominantly of the face-centered cubic (FCC) structure as 80 ± 5% of the atoms are identified as having an FCC-like environment. This result is consistent with what one would expect given that the two metals crystallize in the FCC structure and that there is almost no size mismatch. In terms of composition, the critical nuclei all contain an excess of Pd, relative to the composition of the liquid mixture. We observe some small variations in the average composition of the critical nucleus (e.g., the excess in Pd is 10% for a mole fraction $x_{Pd} = 0.2$ in the liquid mixture and 6% for $x_{Pd} = 0.8$). It seems unlikely, however, that this small difference in the composition of the critical nuclei accounts for such a dramatic change in ΔG_{nucl}.

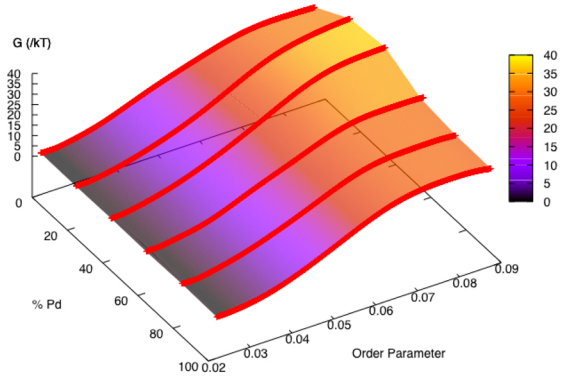

Figure 1. Gibbs free energy profiles of nucleation from liquid Pd−Ag mixtures as a function of the order parameter. For all compositions, the lower end of the order parameter range (left-hand side of the graph) corresponds to the homogeneous liquid mixture. The upper end of the order parameter range (right-hand side of the graph) corresponds to a system containing a crystal nucleus of a critical size. Note the high free energy barrier (shown in bright yellow) obtained for systems with mole fractions of Pd between 0.2 and 0.4.

We now analyze what occurs during the nucleation process, i.e. before the formation of the critical nucleus. Since the only, albeit small, difference we observed pertained to the composition of the critical nucleus, we carefully follow the evolution of the excess in Pd during the nucleation process. We present in Figure 2 the results obtained during the nucleation from liquid mixtures with $x_{Pd} = 0.2$ and $x_{Pd} = 0.8$. Figure 2 shows two very different behaviors. At low Pd mole fractions, nucleation starts with a reorganization of the liquid mixture (Figure 2a, corresponding to values below 0.06 for the order parameter in Figure 1) that results in the formation of a cluster with an excess in Pd of 95% (Figure 2b). In order to identify this mechanism, we examine the structure of the liquid mixture *prior* to the formation of the crystal nucleus. For this purpose, we locate the spherical region of the liquid where the crystal nucleus forms. We present in Figure 2a the Pd−Pd pair correlation function in this region and compare it to the Pd−Pd pair correlation function for the entire liquid mixture. Figure 2a shows that the height of the first peak is increased in the region where the crystal nucleus forms. This increased height is consistent with a short-range demixing effect and with the formation of a liquid region containing an excess in Pd. This leads to the formation of a crystalline cluster with an excess in Pd of 95% (see Figure 2b). These results point toward a local demixing occurring in the early stages of the nucleation process at low Pd mole fractions. As the nucleation process further advances (Figure 2b), the size of the nucleus increases and the excess in Pd in the crystal nucleus decreases until it reaches a value of 10% for the critical nucleus. At high Pd mole fraction, we do not observe any strong demixing and the excess in Pd remains rather stable (between 4% and 8%) throughout the nucleation process, as shown in Figure 2b. We therefore attribute the steep increase in ΔG_{nucl} observed at low Pd mole fractions in the liquid mixture to the local demixing occurring early in the nucleation process.

What is the driving force leading to a local demixing at the beginning of the nucleation process? Why does the nucleation start with the formation of clusters with large excesses in Pd rather than clusters of the thermodynamically stable solid solution? As discussed recently by Kawasaki and Tanaka,[32] prior to crystallization, an undercooled melt should not be seen as a homogeneous disordered phase, but rather as a phase that contains transient, partially organized, domains that act as metastable precursors for the nucleation process. Here, we

dx.doi.org/10.1021/ja500621m | J. Am. Chem. Soc. 2014, 136, 8145−8148

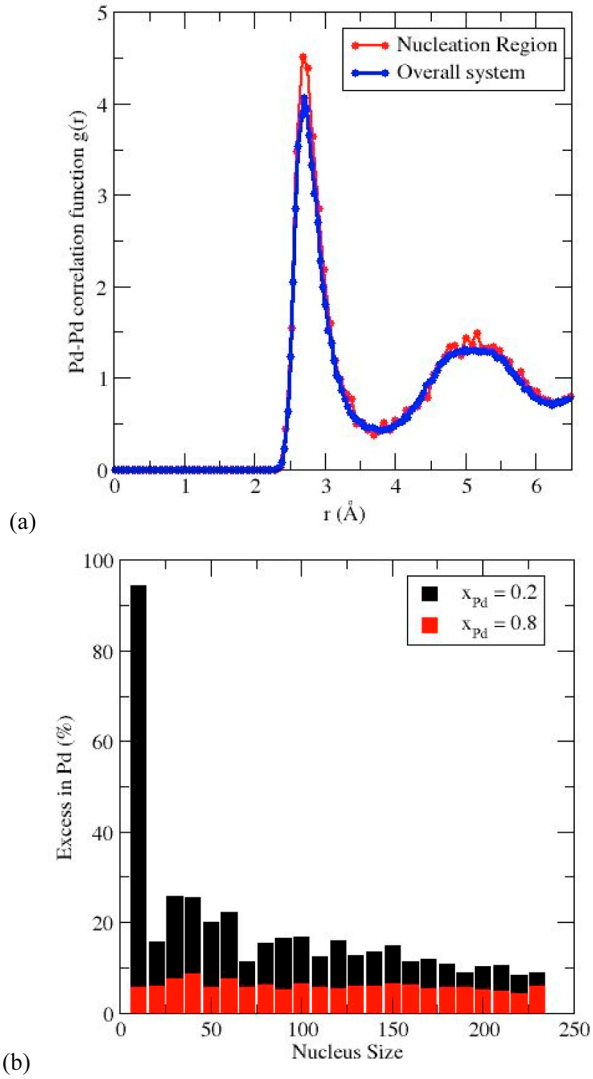

Figure 2. (a) Pd–Pd pair correlation function $g(r)$ in an undercooled liquid mixture with x_{Pd} = 0.2 prior to the formation of the crystal nucleus. The red curve is calculated by taking into account pairs with at least a Pd atom within the nucleation region (i.e., the spherical region of a 1 nm diameter where the crystal nucleus forms), while the blue curve takes into account all Pd pairs within the mixture. (b) Excess in Pd (%) in the crystal nucleus during nucleation. For all liquid compositions, throughout nucleation, the crystal nuclei always contain an excess of Pd. Most notably, for a liquid mixture with x_{Pd} = 0.2 (shown in black), nucleation starts with the formation of nuclei with a large Pd excess of 95% and ends with a critical nucleus containing an excess in Pd of 10%. For a liquid mixture with x_{Pd} = 0.8, the excess in Pd in the crystal nucleus remains between 4% and 8% throughout the nucleation process.

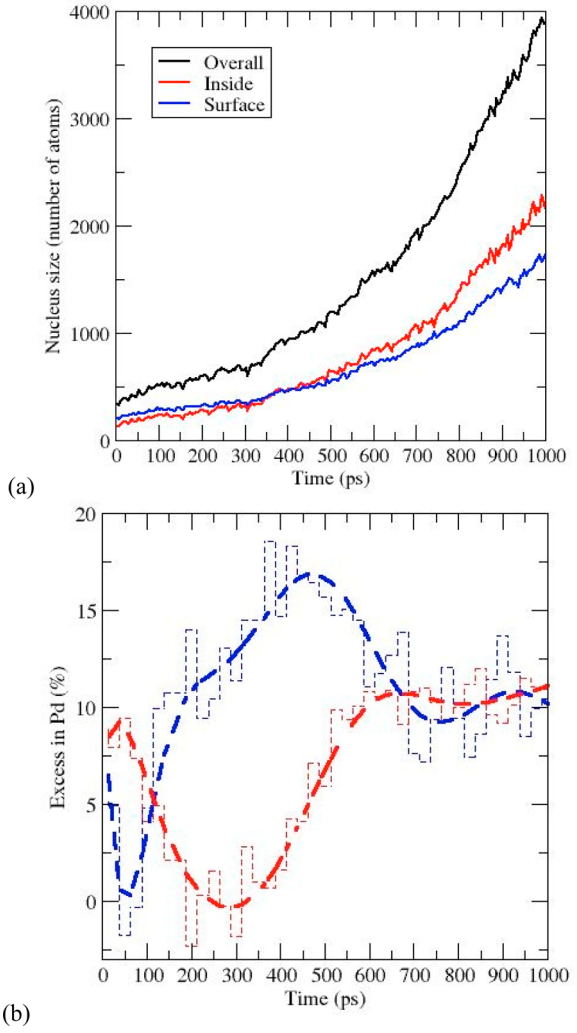

Figure 3. Growth of the crystallite formed from an undercooled liquid mixture with x_{Pd} = 0.2. (a) Time evolution of the total number of atoms contained in the crystallite (in black), including the number of atoms located at the surface of the crystallite (in blue) and the number of atoms located inside the crystallite (in red). (b) Time evolution of the excess in Pd at the surface (in blue) and inside (in red) the crystallite.

obtain crystal nuclei which all exhibit an excess in Pd. This means that, in our case, the role of these metastable precursors to crystal nucleation is played by transient liquid domains, with a large amount of Pd, that form within the undercooled liquid mixure. The formation of these domains can be attributed to the strong cohesion between Pd atoms (see the relative cohesive energies: for Pd, E_{Pd} = 3.89 eV/atom; for Ag, E_{Ag} = 2.95 eV/atom).[21] For liquid mixtures with a low Pd mole fraction, the probability of occurrence of a liquid domain with a large amount of Pd is very low. As a result, we obtain a large ΔG_{nucl} for liquid mixtures predominantly composed of Ag. On the other hand, for mixtures with a high mole fraction in Pd, liquid domains containing a large amount of Pd form very frequently, resulting in a much smaller ΔG_{nucl}.

We turn to the crystal growth process and examine if the interplay between local demixing and crystallization also impacts crystal growth. We focus on the growth process from an undercooled liquid mixture with x_{Pd} = 0.2. To elucidate the growth mechanism, we follow the evolution in size and composition of the crystallite during a crystal growth trajectory (see Figure 3).

We present in Figure 3a the increase in the number of atoms in the crystallite as a result of crystal growth. This provides direct insight in the kinetics of the growth process. The results of Figure 3a show that, within a period of 1 ns, the number of atoms in the crystallite is multiplied by a factor of 10. In terms of dimensions, this corresponds to an increase in the size of the crystallite from roughly 2 to 5 nm within 1 ns. We then separate the atoms belonging to the crystallite into two classes, i.e. the atoms located on the surface of the crystallite and the atoms located inside the crystallite. Figure 3a shows that, throughout the 1 ns window, the contribution of the surface atoms to the

dx.doi.org/10.1021/ja500621m | J. Am. Chem. Soc. 2014, 136, 8145–8148

nanosized crystallite remains strong, as the fraction of surface atoms becomes less than 50% only after 400 ps. We finally present in Figure 3b the time evolution of the excess in Pd at the surface and inside of the crystallite. The time evolution of the excess in Pd at the surface and inside outlines the dramatic variations in the nature of the nanocrystallite as growth proceeds. For instance, after 50 ps, the crystallite is composed of 400 atoms, with a shell that has virtually no excess in Pd while the core of the crystallite shows an excess in Pd of 9%. However, after 300 ps, there are 660 atoms in the crystallite, with a shell showing a notable excess in Pd (12.5%) while the core exhibits no excess in Pd.

Prior work on polymer blends[10−13] has shown that phase separation in mixtures takes place during the growth process only if the diffusion coefficient for one of the components is much larger. To further interpret the results presented in Figure 3, we determine the diffusion coefficients of Ag and Pd in the liquid mixture. We find similar results for the two components (0.71×10^{-9} m^2/s for Ag and 0.8×10^{-9} m^2/s for Pd), which accounts for the fact that no definite phase separation takes place during growth. The growth mechanism observed results from the competition between two effects: (i) the larger cohesive energy of Pd, which tends to lead to a preferential inclusion of Pd atoms in the growing crystal, and (ii) the fast rate of the growth process, which leads to the inclusion of all atoms in the growing crystal, regardless of their nature. The competition between these two effects accounts for the variations observed in the composition of the nucleus at the surface and inside the crystallite (see Figure 3b). We add that, as crystal growth takes place, the atoms located at the surface naturally become part of the inside of the crystallite later on. As a result, the excess in Pd inside the crystallite exhibits the same behavior as the excess in Pd at the surface, with an offset of roughly 250 ps.

Our results show the impact, as well as the persistence, of the coupling between demixing and crystallization throughout the nucleation and growth processes. This interplay leads to an array of complex behaviors, highlighting the ever-changing composition of the crystallite as its size increases. In particular, the crystallization pathway is very much impacted by this interplay, which leads to the formation of crystal nuclei with large excesses (up to 95%) in the component of higher cohesive energy, and results in increases of up to 36 ± 9% in the free energy barrier of nucleation. Our findings also provide a rationalization of how local changes in composition occur at the surface and inside the crystallite. This is especially crucial at the nanoscale, where control of the chemical composition at the surface and inside the particles is key for applications, e.g. in catalysis or in biomineralization processes.[33]

■ ASSOCIATED CONTENT

Ⓢ Supporting Information

A description of the simulation methods, order parameters, and structural analyses. This material is available free of charge via the Internet at http://pubs.acs.org.

■ AUTHOR INFORMATION

Corresponding Author

jerome.delhommelle@und.edu.

Notes

The authors declare no competing financial interest.

■ ACKNOWLEDGMENTS

Partial funding for this research was provided by the National Science Foundation (NSF) through CAREER Award DMR-1052808.

■ REFERENCES

(1) Debenedetti, P. G. *Metastable Liquids. Concepts and Principles*; Princeton University Press: Princeton, 1996.
(2) Mutaftschiev, B. *The Atomistic Nature of Crystal Growth*; Springer-Verlag: Berlin, 2001.
(3) Ostwald, W. *Z. Phys. Chem.* **1897**, *22*, 289.
(4) Davey, R. J.; Schroeder, S. L. M.; ter Horst, J. H. *Angew. Chem., Int. Ed.* **2013**, *52*, 2166.
(5) Bernstein, J. *Polymorphism in Molecular Crystals*; Clarendon Press: Oxford, 2002.
(6) Kurata, R.; Tanaka, H. *J. Phys. Cond. Matt.* **2005**, *17*, L293.
(7) Desgranges, C.; Delhommelle, J. *J. Am. Chem. Soc.* **2011**, *133*, 2872.
(8) Faatz, M.; Gröhn, F.; Wegner, G. *Adv. Mater.* **2004**, *16*, 996.
(9) Wallace, A. F.; Hedges, L. O.; Fernandez-Martinez, A.; Raiteri, P.; Gale, J. D.; Waychunas, G. A.; Whitelam, S.; Banfield, J.; De Yoreo, J. J. *Science* **2013**, *341*, 885.
(10) Tanaka, H.; Nishi, T. *Phys. Rev. Lett.* **1985**, *55*, 1102.
(11) Tanaka, H.; Nishi, T. *Phys. Rev. A* **1989**, *39*, 783.
(12) Shi, W.; Cheng, H.; Chen, F.; Liang, Y.; Xie, X.; Han, C. C. *Macromol. Rapid Commun.* **2011**, *32*, 1886.
(13) Jin, J.; Chen, H.; Muthukumar, M.; Han, C. C. *Polymer* **2013**, *54*, 4010.
(14) Giljohann, D. A.; Seferos, D. S.; Daniel, W. L.; Massich, M. D.; Patel, P. C.; Mirkin, C. A. *Angew. Chem., Int. Ed.* **2010**, *49*, 3280.
(15) Langille, M. R.; Zhang, J.; Personick, M. L.; Li, S.; Mirkin, C. A. *Science* **2012**, *337*, 954.
(16) Agasti, S. S.; Chompoosor, A.; You, C.-C.; Ghosh, P.; Kim, C. K.; Rotello, V. M. *J. Am. Chem. Soc.* **2009**, *131*, 5728.
(17) Sun, S.; Murray, C. B.; Weller, D.; Folks, L.; Moser, A. *Science* **2000**, *287*, 1989.
(18) Ferrando, R.; Jellinek, J.; Johnston, R. L. *Acc. Chem. Res.* **2008**, *108*, 845.
(19) Zheng, H.; Smith, R. K.; Jun, Y.-W.; Kisielowski, C.; Dahmen, U.; Alivisatos, A. P. *Science* **2009**, *324*, 1309.
(20) Rossi, G.; Ferrando, R.; Rapallo, A.; Fortunelli, A.; Curley, B. C.; Lloyd, L. D.; Johnston, R. L. *J. Chem. Phys.* **2005**, *122*, 194309.
(21) Luo, S.-N.; Ahrens, T. J.; Cagin, T.; Strachan, A.; Goddard, W. A.; Swift, D. C. *Phys. Rev. B* **2003**, *68*, 134206.
(22) Kart, H. H.; Tomak, M.; Ulusogan, M.; Cagin, T. *Comput. Mater. Sci.* **2005**, *32*, 107.
(23) ten Wolde, P. R.; Ruiz-Montero, M. J.; Frenkel, D. *Phys. Rev. Lett.* **1995**, *75*, 2714.
(24) Steinhardt, P. J.; Nelson, D. R.; Ronchetti, M. *Phys. Rev. B* **1983**, *28*, 784.
(25) Gasser, U.; Weeks, E. R.; Schofield, A.; Pusey, P. N.; Weitz, D. A. *Science* **2001**, *292*, 258.
(26) Desgranges, C.; Delhommelle, J. *J. Am. Chem. Soc.* **2006**, *128*, 15104.
(27) Desgranges, C.; Delhommelle, J. *J. Am. Chem. Soc.* **2007**, *129*, 7012.
(28) Desgranges, C.; Delhommelle, J. *Phys. Rev. Lett.* **2007**, *98*, 235502.
(29) Punnathanam, S.; Monson, P. A. *J. Chem. Phys.* **2006**, *125*, 024508.
(30) Watson, K. D.; Tatsinkou Nguelo, S. E.; Desgranges, C.; Delhommelle, J. *CrystEngComm* **2011**, *13*, 1132.
(31) Desgranges, C.; Delhommelle, J. *J. Phys. Chem. C* **2009**, *113*, 3607.
(32) Kawasaki, T.; Tanaka, H. *Proc. Natl. Acad. Sci. U.S.A.* **2010**, *107*, 14036.
(33) Raiteri, P.; Gale, J. D. *J. Am. Chem. Soc.* **2010**, *132*, 17623.